ASSESSING AND MODELLING URBAN HEAT ISLAND IN BAGUIO CITY USING LANDSAT IMAGERY AND MACHINE LEARNING

D.C.D.M. Vergara[1], A.C. Blanco[1,2], J.J.S. Marciano Jr.[1], S.F. Meneses III[1], N.J.B. Borlongan[1], A.J.C. Sabuito[1]

[1]Space Information and Infrastructure Bureau, Philippine Space Agency, Quezon City 1101 Philippines
[2]Department of Geodetic Engineering, University of the Philippines Diliman, Quezon City 1101 Philippines
dhann.vergara@philsa.gov.ph, ariel.blanco@philsa.gov.ph, j.marciano@philsa.gov.ph, serafin.meneses@philsa.gov.ph, noel.borlongan@philsa.gov.ph, arlo.sabuito@philsa.gov.ph

Commission IV, WG VII

KEY WORDS: Urban Heat Island, Regression Modelling, UTFVI, LST, NDVI, NDBI

ABSTRACT:

The Urban Heat Island (UHI) is a phenomenon where an urban area experiences higher temperatures than its surroundings. A commonly observed phenomenon worldwide and is one of the serious environmental problems related to urbanization. This paper assessed the past and current state of UHI in Baguio City, the Summer Capital of the Philippines. Land Surface Temperature (LST) layers were generated from Landsat images (March 25, 2019, and March 09, 2022) using the Project GUHeat Toolbox and then used to calculate the Urban Thermal Field Variance Index (UTFVI). The study found out that the UHI has intensified in the past three years. In contrast LST in March 2022 was generally lower than that in March 2019, most likely due to differences in weather conditions. This implies that while it is important to examine the spatiotemporal variations of LST, it is critical that UHI indices are also examined. Random Forest regression was used to examine the UHI indices such as Normalized Difference Built-up Index (NDBI) and Normalized Difference Vegetation Index (NDVI). The explanatory variables used in modelling are (1) NDBI (2) NDVI (3) combination of NDBI and NDVI. The performance of the models is evaluated with Mean Squared Error (MSE) and R-squared (R^2). Using NDBI or NDVI alone yielded a less satisfactory model. The combination of NDBI and NDVI resulted in a good prediction of UHI with R^2=0.89 and MSE=0.006.

1. INTRODUCTION

Urbanization is a rural-to-urban transformation that involves population, land use, economic activity, and culture (McGranahan & Satterthwaite, 2014). More than one-half (56.2%) of the 2020 world's total population is living in urban areas, which is expected to increase to 60.8% in the next decade and 68% by 2050. Urban growth will likely occur in the less developed regions of East Asia, South Asia, and Africa (UN-Habitat, 2020).

Based on a review of the World Bank (2017), the urban population of the Philippines grew by over 50 million in the past five decades and is projected to grow to approximately 102 million by 2050. The high and increasing population of cities gave rise to economic benefits arising from the concentration of business and housing in particular areas that provided many opportunities for structural transformation of the economy. According to the report, while urbanization has positive impacts on economic growth and poverty reduction, the country has not benefited from urbanization gains compared to other countries because of structural issues and binding constraints. Poor land-use planning and limited capacities in property taxes are considered binding constraints related to land administration and management in urban areas of the Philippines. These binding constraints has significant effects on the vibrancy of the land market, in shaping and rationalizing urban growth in a sustainable manner, and in generating revenues to support programs to improve urban life.

Population growth and anthropogenic activities in urban areas contribute to various environmental problems such as altered climate, water, and energy balance, air pollution, and urban heat island (UHI) (Canete et al., 2019; Firozjaei et al., 2022). The UHI is a phenomenon where urban and suburban areas experience warmer temperatures compared to their rural surroundings (Heisler & Brazel, 2010). There are three types of

UHI, namely --- air temperature, subsurface and surface temperature --- which differ in the ways they are formed, and the techniques used to identify and measure them (Oke, 2006).

The air temperature UHI is estimated with the use of air temperature (AT) data acquired in meteorological stations. The use of AT data only represents the specific location, and it is difficult to estimate the temperature variability in mountain areas with AT since the weather is particularly sensitive to small changes in climate forcing (Daly et al., 2008; Rangwala & Miller, 2012). The subsurface UHI is measured in the ground beneath the surface. Lastly, the surface UHI is estimated with remote sensing techniques. The surface UHI is based on the Land Surface Temperature (LST), which is retrieved from thermal infrared (TIR) spectral measurements by airborne or satellite-based sensors (Mutiibwa et al., 2015). The urban thermal field variance index (UTFVI) is used by several papers to estimate UHI (Naim and Kafy, 2021; Sobrino and Irakulis, 2020).

In Baguio City, the UHI value has increased from 1987 to 2015 due to the rapid expansion of impervious surfaces and the loss of green spaces caused by rapid urbanization (Estoque & Maruyama, 2017). The increase in LST values is predicted to intensify the effects of UHI on the city (Baloloy et al., 2019). Future urbanization scenarios were simulated with ENVI-met to assess the effects of urbanization on the microclimate of Baguio City. Scenarios include (1) the current climate, (2) the removal of Balete trees, and (3) removal of some pine trees and addition of new buildings. The models found out that there are 0°C to -

0.01°C temperature differences between the current and simulated conditions (Baloloy et al., 2020).

Monitoring of UHI variation provides useful information in land administration and management in urban areas, which can help in minimizing its impact on human health and the environment. However, the use of ground measurements to assess it had a limitation since meteorological stations are unevenly distributed in most urban areas, especially in densely built-up areas where the UHI effect is intense. To fill the existing data discrepancies, the use of remote sensing techniques has been introduced in different papers (Zhou et al., 2018; Maharjan et al., 2021). Several studies used machine learning techniques like regression to model and predict UHI using the LST as a dependent variable, and different indices as explanatory variables (Zhang et at., 2009; Alcantara et al., 2019).

The study adopted the use of satellite images to assess the past and the current state of UHI in Baguio City and utilized Random Forest regression analysis to predict how UTFVI changes considering the indices NDVI (Normalized Difference Vegetation Index) and NDBI (Normalized Difference Built-up Index).

2. MATERIALS AND METHODS

2.1 Study Area

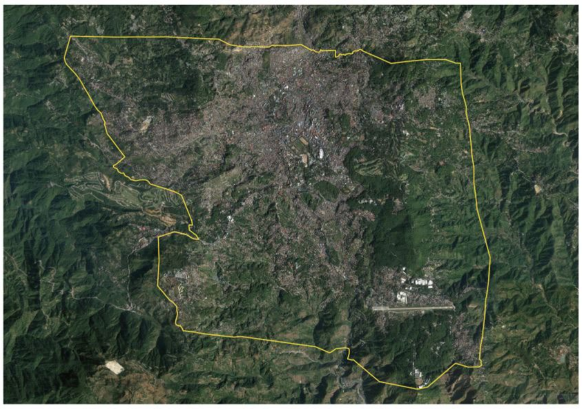

Figure 1. Google satellite image showing the administrative boundary (yellow) of Baguio City

Baguio City is located in the southern part of Benguet Province in the Cordillera Administrative Region (CAR). The city is located on the side of a mountain range, with many hills and plateaus. Several rivers run through the city, including the Bued, Balili, Galiano-Camp-Asin, Naguilian, and Ambalanga. The elevation of the city ranges from 900 meters along the Bued River to 1,600 meters at Pacdal (Baguio City Planning and Development Office, 2018).

The city's land cover is predominantly made up of forested areas, but during the past few decades, these areas have been transformed into residential and commercial areas in response to the city's rapid population growth and economic activities. Being situated on the main island of Luzon, the city is an accessible place for the people who want to relax and escape the excessive heat of the lowland. The city is a famous tourist destination especially during the dry season because of its cool climate and peaceful environment, which makes it a “Summer Capital of the Philippines” (Estoque & Murayama, 2011).

2.2 Data Used

The Landsat 8 and 9 satellite images used in the study are acquired from the USGS Earth Explorer website (https://earthexplorer.usgs.gov/). To get a better result, the study considered the availability of data and selected the images that had no cloud cover. The study chose the month of March since it is the only month in the hot dry season that had no clouds. The Landsat-captured (https://landsat.gsfc.nasa.gov/) images of the city in 2022 are mostly obstructed by clouds for the months of April and May. The highest temperature recorded in the city by the PAGASA Baguio station from 1988-2020 was in March 1988 (PAGASA, 2022). This study therefore focuses on the month of March. The Landsat 8 and 9 data used in the study are captured on March 25, 2019 and March 09, 2022, respectively. These two satellite images were used to calculate the LST, UTFVI, NDVI and NDBI to examine the thermal, vegetation and built-up changes in Baguio City.

The study also used the air temperature data acquired in Philippine Atmospheric Geophysical and Astronomical Services Administration (PAGASA) Baguio Synoptic and Upper-Air station to verify the satellite-derived LST. The PlanetScope (https://www.planet.com/) satellite images give insight into what happened between 2019 and 2022.

2.3 Data Processing

The images are processed using Project GUHeat (http://www.guheat.tcagp.upd.edu.ph/hub.html) toolbox in QGIS to produce spatiotemporal LST maps. The mean of LST outputs are used to calculate the UTFVI of the city.

The satellite images are also used to calculate the NDVI and NDBI. The calculations of these indices are based on the specific properties of the features of interest in terms of absorption and reflection in different spectral bands of multispectral imagery.

The NDVI and NDBI outputs are used as explanatory variables in the regression model to estimate the UTFVI.

2.3.1 Normalized Difference Vegetation Index (NDVI)

NDVI is the most commonly used index for retrieval of vegetation based on surface relative reflectivity in the near infrared (NIR) and Red wavelengths of the spectrum (Carlson et al., 1994). The NDVI is calculated as

$$NDVI = \frac{(NIR - R)}{(NIR + R)} \quad (1)$$

The pixel values of raster produced using the equation is ranging from -1 to 1, which represents the health of vegetation. The high positive values correspond to dense and healthy vegetation cover, while the low positive and negative values indicate non-vegetated areas such as barren land, sand, paved surfaces, and water. (Perez & Comiso, 2014; Zhang et al., 2009).

2.3.2 Normalized Difference Built-up Index (NDBI)

NDBI is used to extract built-up features of the city. The NDBI raster is derived from the short-wave infrared (SWIR) and NIR channels of multiband remotely sensed imagery (Garg et al., 2016). The formula for calculating NDBI is

$$NDBI = \frac{(SWIR - NIR)}{(SWIR + NIR)} \quad (2)$$

The resulting raster will have pixel values ranging from -1 to 1 where higher values are indicators of anthropogenic land surface modification (Canete et al., 2019).

2.3.3 LST Retrieval

The study generated the LST for both years using the Landsat images and Project GUHeat toolbox in QGIS. The methodology used by the toolbox to estimate the LST is from Jeevalakshmi et al. (2017). The method involves converting the band 10 digital number (DN) values to at-sensor spectral radiance and converting them to brightness temperature (BT). Next, the NDVI is computed and used to calculate the proportional vegetation (Pv). The land surface emissivity (LSE) is then derived from Pv and NDVI. Lastly, the calculation of LST using BT of band 10 and LSE.

2.3.4 Urban Thermal Field Variance Index

Urban thermal field variance index was used to quantitatively measure the UHI vulnerability of the area (Alcantara et al., 2019). UTFVI can be calculated using the equation:

$$UTFVI = \frac{T_s - T_{mean}}{T_s} \tag{3}$$

Where, Ts is the LST, Tm is the mean LST of the area.

2.3.5 Regression Modelling

Regression modelling was performed to generate a model that would best predict the UTFVI (dependent variable), from the independent variables such as NDBI and NDVI.

The study utilized random forest (RF) regression which is a supervised machine learning method that builds an ensemble of decision trees from a randomized variant of the tree induction algorithm (Louppe, 2015). The study used the “Forest-based Classification and Regression” toolset in ArcGIS to train models and generate predictions. Three RF models were developed using the Landsat-based (1) NDBI, (2) NDVI, and (3) NDBI-NDVI combinations as explanatory training datasets, along with the UTFVI-based SUHI generated by this study. The models are used to predict SUHI variations and examined using R^2 and MSE to evaluate the overall performance of RF models.

In order to determine which areas were accurately predicted and which areas had under- and over-predictions, the study compared the generated SUHI estimation of three models to the UTFVI-based SUHI.

3. RESULTS AND DISCUSSION

3.1. NDVI and NDBI

Figure 2 shows the variations of NDVI in Baguio City during 2019 and 2022. High NDVI values were mostly found in the forest and underdeveloped areas, while the low NDVI values were found in the business district area. The figure also shows that the grassland and agriculture areas in the 2022 NDVI map are much greener compared to March 2019, which implies that the vegetation is healthier now than it was in 2019.
The NDVI difference map in Figure 2 revealed the growth change of vegetation in Baguio City from 2019 to 2022. The difference values are mostly in the 0.00 to 0.10, which indicates that the vegetation has increased in the current year.

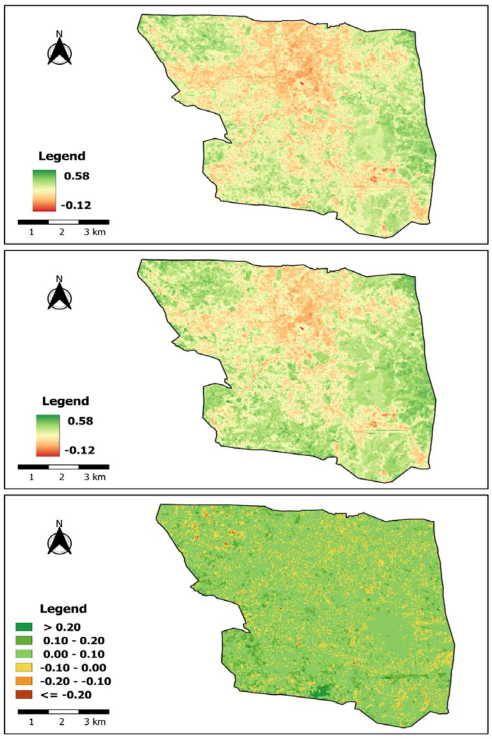

Figure 2. Spatial distributions of NDVI in Baguio City in 2019 (top) and 2022 (middle), and the difference (bottom). The figure illustrates that the grassland and agriculture areas in the current year are substantially greener than they were in 2019.

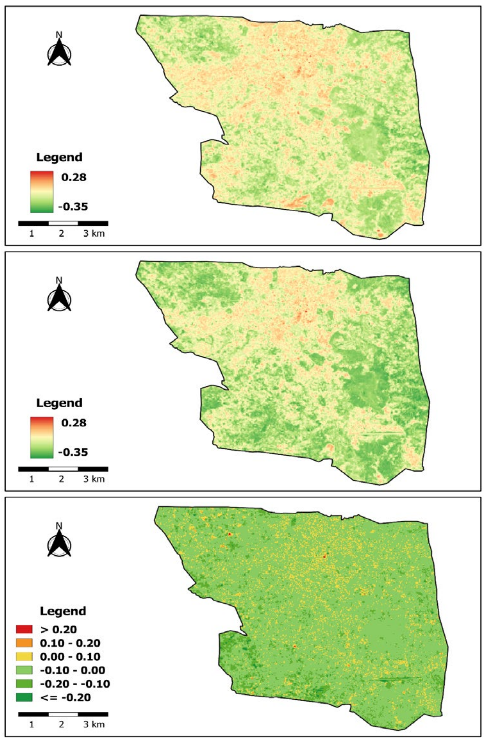

Figure 3. Spatial distributions of NDBI in Baguio City in 2019 (top), 2022 (middle), and the difference (bottom). There are little to minimal changes in impervious surfaces between 2019 and 2022, and the new buildings are still built in the central district of the city. It is also easy to distinguish the built-up pattern in 2022 because of the high contrast or greener vegetation during the same year.

Figure 3 presents the NDBI variations in Baguio City. Even though the NDBI values became lower during 2022 in the vegetative area of the city, the built-up pattern remained the same. High NDBI values are still prominent in the business district area where residential and commercial structures were built, while low values are observed in the forest and active agricultural areas.

Figure 3 (bottom) shows that the difference values are mostly in the -0.10 to 0.00, which indicates that there is minimal change in the built-up areas of the city. It also revealed a pattern of building activities being centered in the business districts of the city.

3.2 LST

The spatial distributions of LST during 2019 and 2022 in Baguio City are shown in Figure 4. The figure revealed that the city experienced much higher LST in 2019 than 2022. Based on Table 1, the air temperature (AT) measurements acquired in PAGASA Baguio Station correspond to the LST values derived from Landsat images. The AT and LST values are both high during March 2019 compared to the March of the current year.

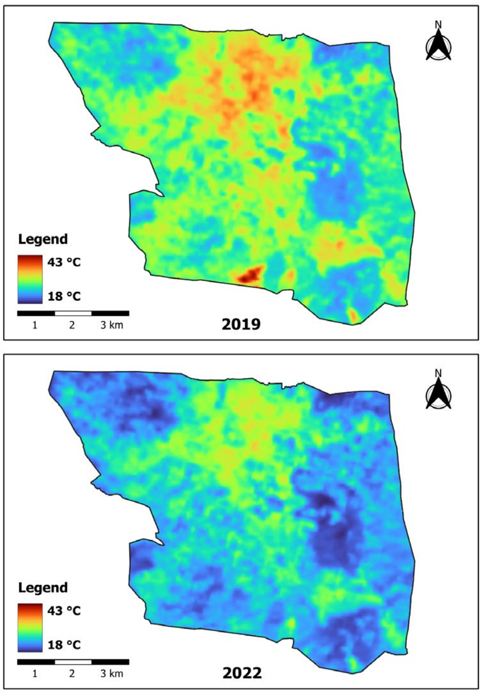

Figure 4. LST distribution in Baguio City on March 25, 2019 and March 09, 2022. The LST values are lower in March 2022 than in March 2019.

Date	ATmax	ATmin	ATmean	LSTmean
March 25, 2019	25.6	13.2	19.4	28.6
March 09, 2022	25.4	12.9	19.2	24.9

Table 1. Air temperature values recorded in PAGASA Baguio Station and LST values during March 2019 and March 2022.

The map also shows that there is an intense LST in the bottom part of the city during March 2019. The pattern observed was also observed in LST maps produced in the previous study of (Project GUHeat, 2020) for the month of April 2019.

The NDBI 2019 output shows intense positive values in that area while NDVI 2019 shows high negative values. Meaning the high LST values in that area are caused by impervious surfaces and lack of vegetation. With the use of PlanetScope satellite images (fig. 4), the study found out that the high LST values are caused by burned vegetation in that year.

In general, the high values of LST are prominent in the industrial area of Baguio City. The dense houses and buildings contribute to the warming of the area that result in an increase in LST (Hua et al., 2020; Yu & Lu. 2014). Therefore, the LST in the industrial area is higher than those of the surroundings.

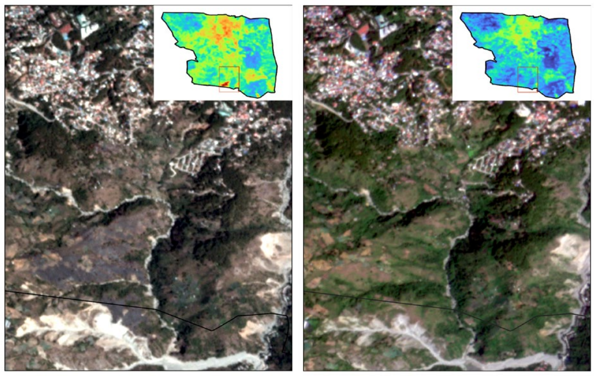

Figure 5. PlanetScope images on March 25, 2019 (left) and March 09, 2022 (right). The left image shows the presence of burned vegetation in the southern part of the city that resulted in high LST values.

3.3 UTFVI-based UHI

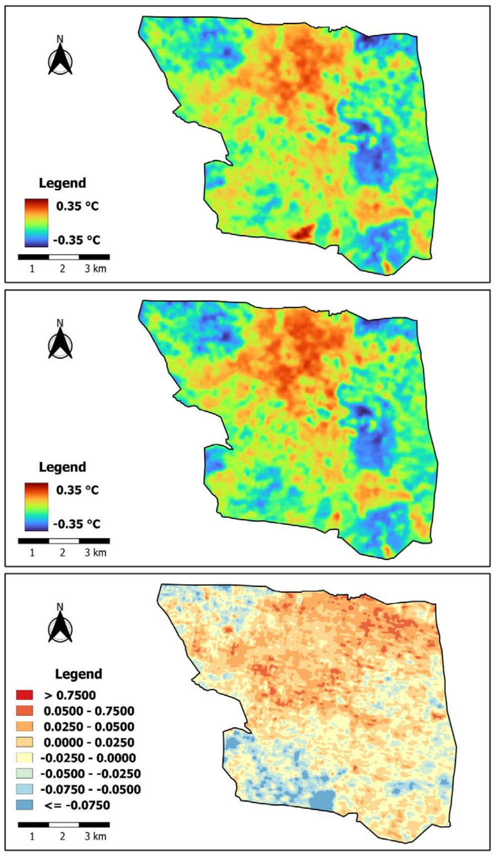

Figure 6. Spatial variations of UTFVI in Baguio City on March 25, 2019 (top) and March 09, 2022 (middle), and the difference (bottom) between them. The UHI effect in the city has increased in the current year, particularly in the central business area.

Figure 6 shows the distribution of UHIs in Baguio City over the study period. As can be seen, the UHI intensity of the city was increased from 2019 to 2022. In general, the UHI hotspots mainly occurred in the business district area of the city, which contains dense urban villages and commercial establishments. The bottom map of Figure 6 revealed that the difference values are mostly in the range of 0.00 to 0.05 degree Celsius, which means most parts of the city experienced an increased UHI intensity. It also shows that the upper and middle parts of the city experienced an increase in UHI intensity.

The output of LST and UTFVI indicates that even if the LST intensity is decreasing the UHI can still possibly increase. So, the modeling of LST as a factor of different indices to predict UHI can be problematic (i.e., no inherent correlation can be derived). Given this scenario, the study tried to model the UHI (UTFVI-based) as a factor of NDBI and NDVI.

3. 4. Random Forest

The combination of NDVI and NDBI as explanatory variables resulted in 0.006 MSE and 0.89 R-squared. The model that used the NDBI as explanatory variable alone resulted in 0.007 MSE and 0.76 R-squared. The model that used the NDVI as explanatory variable alone resulted in 0.009 MSE and 0.72 R-squared. Table 2 summarizes the performance of the models for the cases considered in this study.

MODEL	VARIABLES	MSE	R-SQUARED
1	NDBI	0.007	0.76
2	NDVI	0.009	0.72
3	NDBI & NDVI	0.006	0.89

Table 2. Performance of the random forest regression models considering NDBI and/or NDVI.

The Mean Squared Error (MSE) tells how close the predicted values are to observed values. A good model should have a relatively low MSE value whose ideal value is closer to zero (Das et al., 2004). On the other hand, the R-squared is the proportion of variance in the dependent variable which is explained by the explanatory variables (Miles & Shevlin, 2000).

Figure 6 shows the visual representations of observed UTFVI values against model-predicted values. The scatter plot of NDBI shows that most of the predicted UTFVI of the model are excessively and underrated. For the NDVI model, the predicted values are mostly underestimated. The scatter plot of the NDBI-NDVI combination model shows near prediction results compared to other models. However, some predicted values of the model are also overestimated and underestimated.

Figure 7 shows the actual UTFVI and the predictions made by regression models. As compared to the UTFVI, the predicted output of the NDVI-NDBI combination model is the best model to predict UHI. Its prediction shows a similar pattern of observed UTFVI hotspots and coldspots. The NDBI model vividly detects the UHI in the area where impervious surfaces are dense, but struggle in the vegetation areas. For the NDVI model, the predicted values are almost the same in the NDBI model but this model can minimally detect the UHI in the vegetation areas.

The study assessed the accuracy of prediction values to the observed UTFVI by getting the difference or bias of the two variables. Figure 8 shows the difference between observed UTFVI and RF-predicted UTFVI. The values that are closer to 0 show excellent UTFVI estimate. In the visualization, the yellow color ranges from 0.00 to 0.05 values. As a result, the more yellow the model is, the closer it estimates the UTFVI. The figure also shows that overestimated values are mostly in areas with dense impervious surfaces, while underestimated values are found in vegetation areas.

Figure 9 shows how the observed NDBI and NDVI affected the biases in model predictions. For NDBI, the biases are expected in negative NDBI values. While in NDVI, the biases are in positive NDVI values. In general, the vegetation areas are more likely to have overprediction and underprediction of UHI.

These results show that the best model to predict UHI is the model 3 (NDBI-NDVI combination) since it has the lowest MSE (0.006) and highest R-squared (0.89) values, and it also shows similar patterns of hotspots and coldspots of UHI.

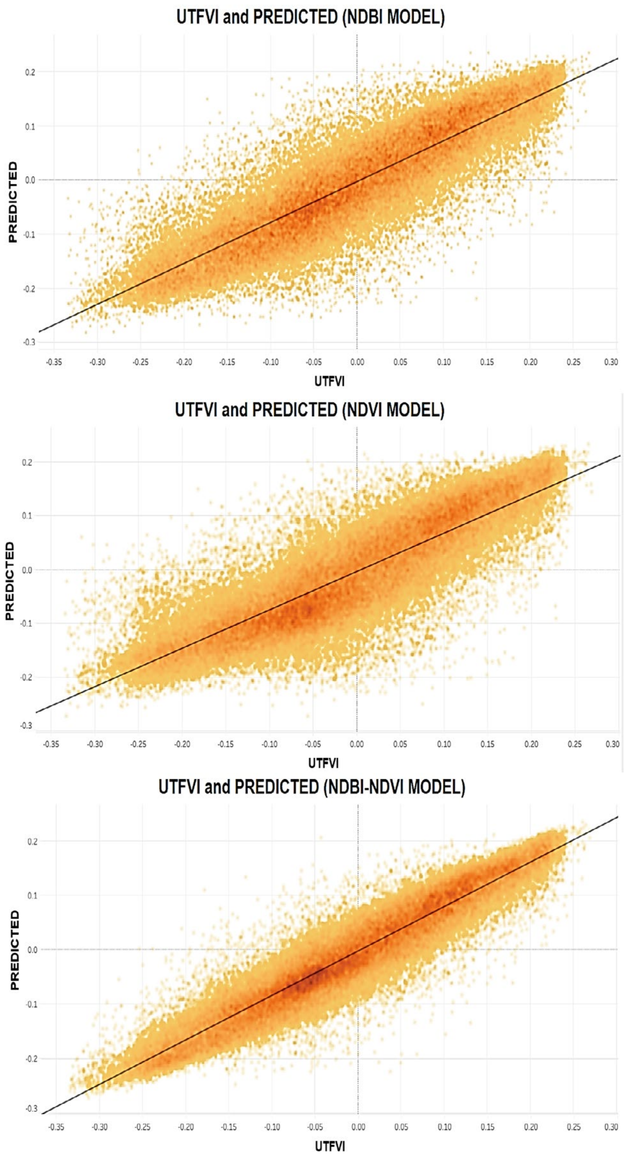

Figure 6. Scatter plots of UTFVI and RF-predicted UTFVI using NDBI (top), NDVI (middle), and NDBI-NDVI (bottom). Using both NDBI and NDVI results in less scatter of points with respect to the fitted line.

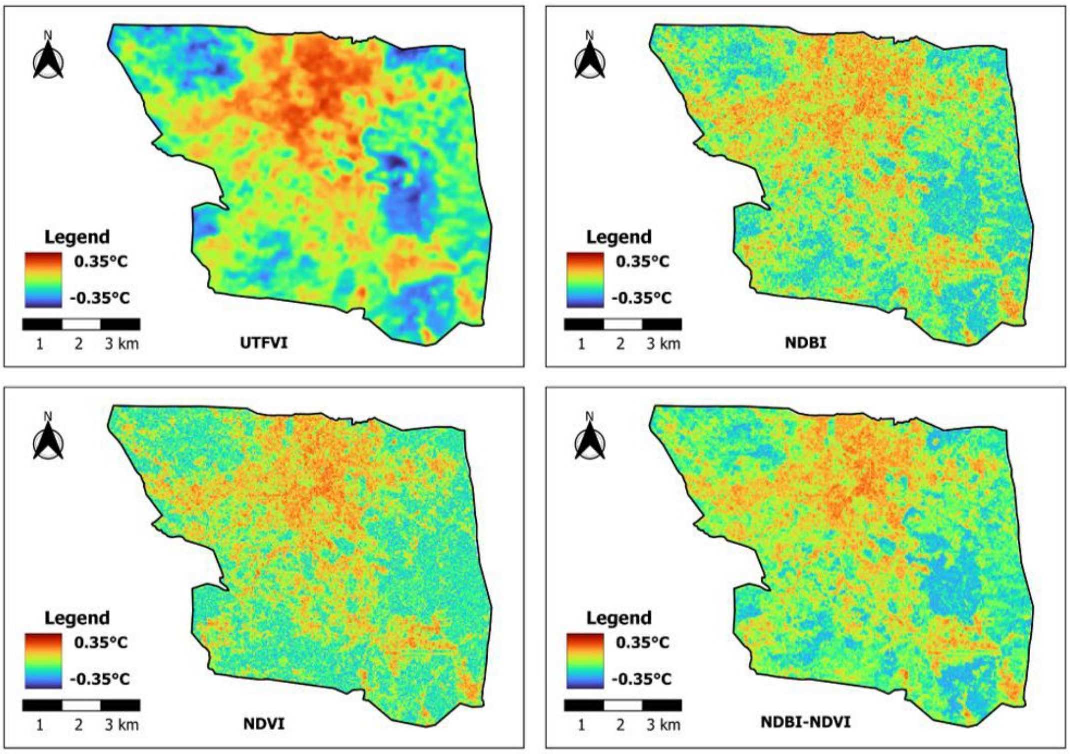

Figure 7. Comparison of observed and predicted UTFVI. The RF models were able to predict the UTFVI intensity especially in the built-up areas. However, some values in certain areas are overestimated while others are underestimated.

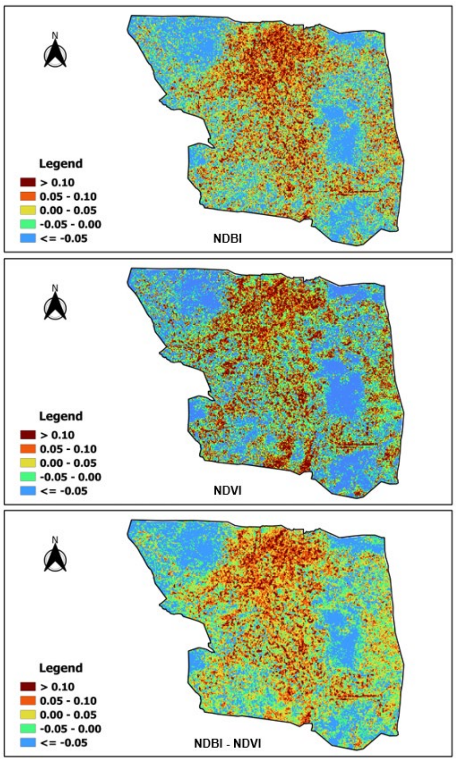

Figure 8. The figure shows the difference between observed and R-F predicted UTFVI values. The figure revealed that overestimated values are usually found in impervious surfaces, whereas underestimated values are mostly found in vegetation areas. A more accurate prediction is obtained when the NDBI and NDVI indices are combined as input data for modelling.

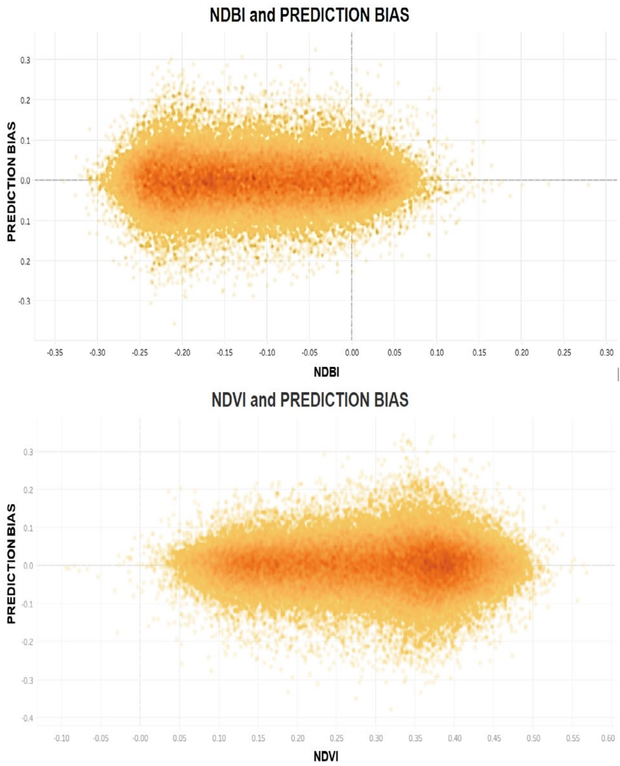

Figure 9. Distribution of prediction bias in relation to NDBI and NDVI observed values. The scatter plots revealed that vegetation areas are more likely to have overprediction and underprediction of UHI.

4. CONCLUSION

Regarded as the "Summer Capital of the Philippines", Baguio city is a popular tourist destination for people who want to escape the heat in the lowland areas in the Philippines. The results of UTFVI analysis, however, point to worsening surface UHI phenomenon in Baguio City in the past three years due to an increase in built-up areas. On the other hand, the LST layers showed that March 2022 was cooler than March 2019. This contrasts with the findings based on UTFVI. LST alone is not always a good indicator of UHI as surface temperatures are affected by weather conditions. Based on the results of regression analysis using Random Forest, the NDBI-NDVI combination model proposed and used in this study can account for about 89% of the variation in UTFVI. The output of this study can provide useful information in city planning and development as well as in policymaking to improve environmental conditions of the city.

ACKNOWLEDGEMENT

The researchers would like to extend their gratitude to USGS, Google Earth, and PlanetScope for the satellite images, and PAGASA for the synoptic weather data that were used in this study.

REFERENCES

Alcantara, C.A., Escoto, J.D., Blanco, A.C., Baloloy, A.B., Santos, J.A., Sta. Ana., R.R, 2019. Geospatial assessment and modeling of urban heat islands in Quezon city, Philippines using OLS and geographically weighted regression.

Baguio City Planning and Development Office, 2018. Baguio City Ecological Profile, 2018.

Baloloy, A., Sta. Ana, R.R., Cruz, J.A., Blanco, A., Lubrica, N.V., Valdez, C.J., Cajucom, E.P., 2020. Spatiotemporal multi-satellite biophysical data analysis of the effect of urbanization on land surface and air temperature in Baguio City, Philippines. The International Archives of the Photogrammetry, Remote Sensing and Spatial Information Sciences, Volume XLII-4/W19, 2019. PhilGEOS x GeoAdvances 2019.

Baloloy, A., Cruz, J.A., Sta. Ana, R.R., Blanco, A., Lubrica, N.V., Valdez, C.J., Bernardo, J.J., 2020. Modelling and simulation of potential future urbanization scenarios and its effect to the microclimate of Lower Session Road, Baguio City. ISPRS Annals of the Photogrammetry, Remote Sensing and Spatial Information Sciences, Volume V-4-2020, 2020. XXIV ISPRS Congress (2020 edition).

Carlson, T. N., Gillies, R. R., Perry, E. M., 1994: A method to make use of thermal infrared temperature and NDVI measurements to infer surface soil water content and fractional vegetation cover. Remote Sensing Reviews 9(1-2), 161-173.

Canete, S.F., Schaap, L.L., Andales, R., Otadoy, R.E.S., Blanco, A., Babaan, J., Cruz, C., 2019. Analysis of the impact of vegetation distribution, urbanization, and solar radiation on the seasonal variation of the urban heat island effect in Cebu city using landsat and global horizontal irradiance data.

Daly, C., Halbleib, M., Smith, J.I., Gibson, W. P., Doggett, M. K., Taylor, G. H., Curtis, J., and Pasteris, P. P., 2008. Physiographically sensitive mapping of climatological temperature and precipitation across the conterminous United States. Int. J. Climatol., 28, 2031–2064, https://doi.org/10.1002/joc.1688

Das, K., Jiang, J., Rao, J., 2004. Mean squared error of empirical predictor. Annals of Statistics, 32. 10.1214/009053604000000201.

Estoque, R.C., Murayama, Y., 2011. City Profile: Baguio. Cities 30: 240-251. 10.1016/j.cities.2011.05.002

Estoque, R.C., Murayama, Y., 2011. Spatio-Temporal Urban Land Use/Cover Change Analysis in a Hill Station: The Case of Baguio City, Philippines. Procedia - Social and Behavioral Sciences, Volume 21, 2011, Pages 326-335, ISSN 1877-0428, https://doi.org/10.1016/j.sbspro.2011.07.016.

Estoque, R.C., Murayama, Y., 2017. Monitoring surface urban heat island formation in a tropical mountain city using Landsat data (1987–2015). ISPRS J Photogramm. pp18-29.

Firozjaei, N.K., Kiavarz, M., Alavipanah, S.K., 2022. Quantification of landscape metrics effects on downscaled urban land surface temperature accuracy of satellite imagery. Advances in Space Research. doi.org/10.1016/j.asr.2022.04.021 0273-1177/Ó 2022

Garg, A., Pal, D., Singh H., Pandey, D.C., 2016. "A comparative study of NDBI, NDISI and NDII for extraction of urban impervious surface of Dehradun (Uttarakhand, India) using Landsat 8 imagery," 2016 International Conference on Emerging Trends in Communication Technologies (ETCT), 2016, pp. 1-5, doi: 10.1109/ETCT.2016.7882963.

Heisler, Gordon M.; Brazel, Anthony J. 2010. The urban physical environment: temperature and urban heat islands Chapter 2. In: Aitkenhead-Peterson, Jacqueline; Volder, Astrid, eds. Urban Ecosystem Ecology. Agronomy Monograph 55. Madison, WI: American Society of Agronomy, Crop Science Society of America, Soil Science Society of America: 29-56.

Hua, L., Zhang, X., Nie, Q., Sun, F., Tang, L., 2020. The Impacts of the Expansion of Urban Impervious Surfaces on Urban Heat Islands in a Coastal City in China. Sustainability, MDPI, vol. 12(2), pages 1-21, January.

Jeevalakshmi, D., Narayana Reddy, S., Manikiam, B., 2017. Land Surface Temperature Retrieval from Landsat data using Emissivity Estimation. International Journal of Applied Engineering Research. Vol. 12, No. 20. 9679-9687.

Louppe, G., 2015. Understanding random forests from theory to practice.

Maharjan, M., Aryal, A., Man Shakya, B., Talchabhadel, R., Thapa, B.R., Kumar, S, 2021. Evaluation of Urban Heat Island (UHI) Using Satellite Images in Densely Populated Cities of South Asia. Earth 2021, 2, 86–110. https://doi.org/10.3390/earth2010006.

McGranahan, G., Satterthwaite, D., 2014. Urbanisation concepts and trends. IIED Working Paper. International Institute for Environment and Development, London.

Miles, J., Shevlin, M., 2000. Applying regression and correlation: a guide for students and researchers.

Mutiibwa, D., Strachan, S., Albright, T., 2015. Land surface temperature and surface air temperature in complex terrain.

Naim, M.N.H., Kafy, A.A., 2021. Assessment of urban thermal field variance index and defining the relationship between land cover and surface temperature in Chattogram city: A remote sensing and statistical approach, Environmental Challenges, Volume 4, 2021, 100107, ISSN 2667-0100, https://doi.org/10.1016/j.envc.2021.100107.

Oke, T.R., 2006. Towards better communication in urban climate. Theoretical and Applied Climatology, 84:179–189.

Perez, G.J.P., and Comiso, J.C., 2014. Seasonal and interannual variabilities of Philippine vegetation as seen from space. Philippine Journal of Science, 143(2), 147-155.

Philippine Atmospheric Geophysical Astronomical Services Administration, 2022. Climatological Extremes: Baguio City, Benguet as of 2020. Retrieved https://pubfiles.pagasa.dost.gov.ph/pagasaweb/files/cad/CLIMATOLOGICAL%20EXTREMES%20(as%20of%202020)/Baguio.pdf#toolbar=0&navpanes=0 June 01, 2022.

Philippine Atmospheric Geophysical Astronomical Services Administration, 2022. Daily weather data measured in the PAGASA – Baguio Station for the month of March (2019-2022).

Rangwala, I., & Miller, J., 2012. Climate change in mountains: A review of elevation dependent warming and its possible causes. Climatic Change, vol. 114, pp. 527–547, 2012, doi:10.1007/s10584-012-0419-3

Sobrino, J.A.; Irakulis, I. A Methodology for Comparing the Surface Urban Heat Island in Selected Urban Agglomerations Around the World from Sentinel-3 SLSTR Data. Remote Sens. 2020, 12, 2052. https://doi.org/10.3390/rs12122052.

UN-Habitat, 2020. World cities report 2020: The value of sustainable urbanization. United Nations Human Settlements Programme (UN-Habitat).

World Bank, 2017. Philippines Urbanization Review: Fostering Competitive, Sustainable and Inclusive Cities. World Bank, Washington, DC. © World Bank. https://openknowledge.worldbank.org/handle/10986/27667 License: CC BY 3.0 IGO

Yu, X., Lu, C., 2014. Urban percent impervious surface and its relationship with land surface temperature in Yantai City, China. IOP Conference Series: Earth Environmental Science. 17 (2014) 012163

Zhang, Y., Odeh, I.O.A., Han, C., 2009. Bi-temporal characterization of land surface temperature in relation to impervious surface area, NDVI, and NDBI, using a sub-pixel image analysis.